DOI: 10.1002/ejic.201001197

Synthesis and Application of New Guanidine Copper Complexes in Atom Transfer Radical Polymerisation

Olga Bienemann,[a] Roxana Haase,[b] Anton Jesser,[a] Tanja Beschnitt,[b] Artjom Döring,[c] Dirk Kuckling,[c] Ines dos Santos Vieira,[a] Ulrich Flörke,[b] and Sonja Herres-Pawlis*[a]

Dedicated to Prof. Bernhard Lippert on the occasion of his 65th birthday

Keywords: Copper / Polymerization / Styrene / Density functional calculations

The synthesis and copper coordination of the ligands TMGd^{i}pae (**L1**) and DMEGd^{i}pae (**L2**) is reported. The solid-state structures of obtained copper complexes [Cu(TMGd^{i}pae)Cl] (**C1**), [Cu(TMGd^{i}pae)Br] (**C2**), [Cu(TMGd^{i}pae)I] (**C3**), [Cu(DMEGd^{i}pae)Cl] (**C4**), [Cu(DMEGd^{i}pae)Br] (**C5**) and [Cu(DMEGd^{i}pae)I] (**C6**) show a trigonal distorted [2+1] coordination of the copper atom and indicate interesting binding properties of aliphatic guanidine hybrid ligands. DFT analysis and calculation of the intramolecular charge transfer by NBO studies allow for a deeper insight into the binding competition between guanidine, amine and halide donor at copper(I). Tetramethylguanidine units act as stronger donors than dimethylethyleneguanidine units. Both ligands in combination with CuCl and CuBr were screened with regard to their activity in atom transfer radical polymerisation of styrene in bulk and in MeCN solution. The polymerisation occurs very fast and has good control. Kinetic studies on the best-behaving system (2TMGd^{i}pae/CuBr) evidence that controlled radical polymerisation occurs until a conversion of 70 % and a polymerisation time of 100 min, after this a deviation towards higher molecular weights can be observed.

Introduction

Cu^I complexes serve as catalysts for a great variety of reactions in academic and industrial synthesis, e.g. in O_2 activation,[1] cyclopropanation of olefins,[2] aziridination,[3] click reactions,[4] atom transfer radical addition (ATRA)[5] and atom transfer radical polymerisation (ATRP),[6] to name but a few. A thorough comprehension of the binding modes in these copper complexes is crucial for the control of the catalytic activity and for the understanding of mechanistic features. In several of the named applications, copper is coordinated by polydentate nitrogen donor ligands.[1–6] Among the numerous N donor ligands studied so far, guanidines represent a rather young ligand class, which has been investigated with the main focus on copper coordination chemistry.[7–10] Generally, guanidines have proven to be powerful N donor ligands in coordination chemistry.[11–15] They should also be suitable for application in ATRP because of three reasons: (i) strong complexation of the transition metal (copper), (ii) stabilisation of the higher oxidation state of the transition metal and (iii) tunable redox potentials of the guanidine complexes.[7–15]

Atom transfer radical polymerisation (ATRP) was developed in 1995 and has considerably widened the field of accessible polymeric materials.[16] The basis of ATRP as a controlled radical polymerisation is an equilibrium between a dormant species, commonly an alkyl or aryl halide, and the propagating radical (Scheme 1). As the equilibrium is strongly shifted to the left, the concentration of free radicals is very low and the contribution of termination reactions is insignificant.

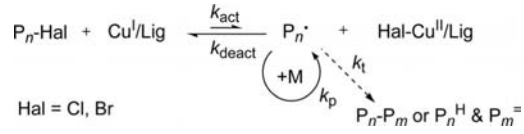

Scheme 1. Overall equilibrium of copper-mediated atom transfer radical polymerisation (ATRP).

The activation of dormant species is mediated by a transition-metal complex: the complex undergoes a one-electron oxidation concomitant with halogen transfer. In comparison with ruthenium- and iron-mediated ATRP, copper-mediated ATRP is most powerful and efficient.[17] It can be

[a] Institut für Anorganische Chemie II der Technischen Universität Dortmund,
Otto-Hahn-Str. 6, 44227 Dortmund, Germany
Fax: +49-231/755-5048
E-mail: sonja.herres-pawlis@tu-dortmund.de
[b] Department Chemie der Universität Paderborn, Anorganische Chemie,
Warburger Str. 100, 33098 Paderborn, Germany
[c] Department Chemie der Universität Paderborn, Organische und Makromolekulare Chemie,
Warburger Str. 100, 33098 Paderborn, Germany
Supporting information for this article is available on the WWW under http://dx.doi.org/10.1002/ejic.201001197.

shown that a good ATRP system possesses several important properties: (i) good donor strength of the ligand for stabilisation of both oxidation states, (ii) high affinity towards halides and (iii) the activator complex should be more reducing. Scheme 2 summarises the most efficient ligands used in ATRP. Though a wide range of ligands has been investigated in copper-mediated ATRP, where nitrogen donors allowed to perform excellent polymerisation control, the development of new catalytic systems is of huge interest.[18]

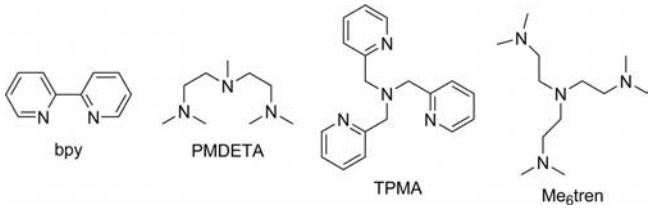

Scheme 2. Most efficient ligands in copper-mediated ATRP.[6]

Until now, the guanidines bis(*N*,*N*,*N*′,*N*′-tetramethylguanidino)ethane and N^1,N^2-bis(1,3-dimethylimidazolin-2-ylidene)ethane-1,2-diamine and the unsaturated bisguanidine derivative 1,2-bis(1,3-diisopropyl-4,5-dimethylimidazolin-2-imino)ethane displayed moderate control in ATRP,[19] which is in contrast to their excellent ligand properties. This contrast between ligand properties and low activity in ATRP can be explained by the huge steric encumbrance of the guanidine moiety, which results in a saturated coordination sphere and blocks halogen transfer.

Herein we report the synthesis of the heterobidentate nitrogen donor ligands 2-[2-(diisopropylamino)ethyl]-1,1,3,3-tetramethylguanidine (TMGd^{i}pae, **L1**) and N^1-(1,3-dimethylimidazolidin-2-yliden)-N^2,N^2-diisopropylethan-1,2-diamine (DMEGd^{i}pae, **L2**), which belong to the group of guanidine hybrid ligands that combine a guanidine and an amine group (Scheme 3).[8d]

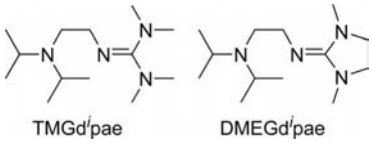

Scheme 3. Ligands **L1** and **L2**.

By single-crystal X-ray structure analysis, we obtained the structures of different halide copper complexes, **C1** to **C6**, which exhibit interesting [2+1] coordinational motifs. These structures allow for a deeper insight into the donor ability of the guanidine hybrid ligands. We examined the resulting trends in the solid-state structures by density functional theory (DFT) and were successful in the elucidation of the binding situation by complex orbital analysis.

The intention of combining an amine with a guanidine moiety in a ligand was to create a catalytic system for ATRP in which strong complexation of the transition metal and a flexible coordination sphere is enabled by the ligand. To probe the activity of catalytic systems consisting of **L1**/**L2** and CuCl/CuBr, we performed styrene polymerisation and kinetic studies on the best system. As a result, we were able to correlate the catalytic activity with ligand donor properties.

Results and Discussion

Synthesis and Characterisation of the Ligands

The substance 2-[2-(diisopropylamino)ethyl]-1,1,3,3-tetramethylguanidine (TMGd^{i}pae, **L1**) was first reported in a patent in 2000 by Kenichi in connection with silver halide photogenic materials.[20] Our contribution presents a synthesis that enables production of **L1** in gram scale and a variation of the guanidine moiety, for example, to 1,3-dimethylimidazolidin-2-ylidene. Both of these criteria are offered by a condensation reaction of a Vilsmeier salt with a primary amine under presence of an auxiliary base, which was developed by Kantlehner.[21] According to this method the aliphatic hybrid ligands 2-[2-(diisopropylamino)ethyl]-1,1,3,3-tetramethylguanidine (TMGd^{i}pae, **L1**) and N^1-(1,3-dimethylimidazolidin-2-yliden)-N^2,N^2-diisopropylethan-1,2-diamine (DMEGd^{i}pae, **L2**) can be synthesised with the corresponding Vilsmeier salts, *N*,*N*,*N*′,*N*′-tetramethylchloroformamidinium chloride (TMG, **L1**) and *N*,*N*′-dimethylethylenechloroformamidinium chloride (DMEG, **L2**) and the amine 2-(diisopropylamino)ethylamine (Scheme 4) in yields of up to 86%. The Vilsmeier salts were prepared according to a literature procedure.[21]

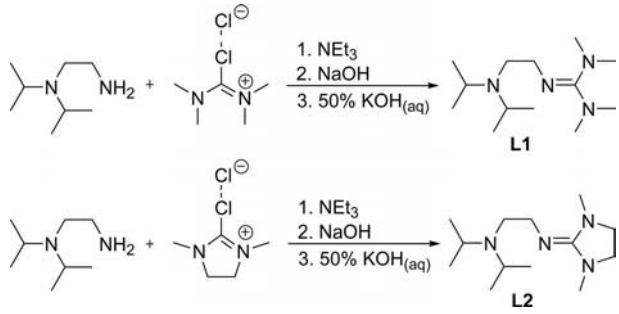

Scheme 4. Synthesis of **L1** and **L2**.

The ligands were fully characterised by NMR and IR spectroscopy and ESI-MS. The presence of the characteristic guanidine carbon atom was confirmed by the signal at 157–162 ppm in the ^{13}C NMR spectrum and the bands for the C=N vibration at 1666 and 1624 cm^{-1} in the infrared spectrum.

Synthesis and Structure of Mononuclear Copper(I) Complexes

The Cu^I complexes [Cu(**L**)X] can be synthesised by reaction of guanidine amine hybrid ligands (**L1**, **L2**) with anhydrous Cu^I salts in dry solvents such as MeCN or THF in good yields of 60–85%. By gas phase diffusion of diethyl ether or diisopropyl ether, crystalline products can be ob-

tained. We successfully crystallised the cpper halide series with both ligands TMGd^{i}pae (**L1**) and DMEGd^{i}pae (**L2**), the mononuclear Cu^I complexes [Cu(TMGd^{i}pae)Cl] (**C1**), [Cu(TMGd^{i}pae)Br] (**C2**), [Cu(TMGd^{i}pae)I] (**C3**), [Cu(DMEGd^{i}pae)Cl] (**C4**), [Cu(DMEGd^{i}pae)Br] (**C5**) and [Cu(DMEGd^{i}pae)I] (**C6**) (Scheme 5).

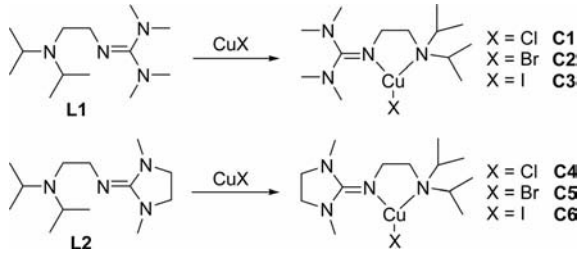

Scheme 5. Synthesis of **C1**–**C6**.

The neutral complexes **C1**–**C6** crystallise in the monoclinic space group $P2_1/c$ (**C1**–**C5**) and $C2/c$ (**C6**). The molecular structures of the complexes are shown in Figure 1, the most important structural data are given in Table 1. The copper(I) atom is coordinated by one chelate ligand and one halide ion in a distorted trigonal-planar manner. The sum of the angles surrounding the Cu^I atom is 359.9 (**C1**), 360.0 (**C2**), 359.9 (**C3**), 359.7 (**C4**), 359.7 (**C5**) and 359.4° (**C6**). A regular trigonal-planar coordination geometry with angles of 120° (ideal) is not possible because of the ligand bite angle N–Cu–N of 79–85°. In the halide series with each ligand, an elongation of Cu–X bond lengths going from chloride to iodide can be found, which is expected with regard to the halide radii. The Cu–N_{gua} bonds in the complexes with **L1** [1.906(1) **C1**, 1.924(2) **C2**, 1.945(2) Å **C3**] are shorter than in the complexes with **L2** [1.937(1) **C4**, 1.950(2) **C5**, 1.982(1) Å **C6**], which indicates a stronger donor ability of the TMG guanidine moiety. In all complexes, the Cu–N_{gua} bond lengths are significantly shorter than the respective Cu–N_{amine} bonds [2.639(1) **C1**, 2.460(2) **C2**, 2.332(2) **C3**, 2.311(1) **C4**, 2.267(2) **C5**, 2.233(1) Å **C6**], which is caused by the stronger σ-donor character of the guanidine function. In complexes **C4** to **C6**, the Cu–N_{amine} coordination is stronger than in complexes **C1** to **C3** because of decreased donor ability of the DMEG guanidine moiety. A comparison of the Cu–X and Cu–N_{amine} distances shows that the decrease in the bond strength between Cu^I and halide ($Cl^- \rightarrow I^-$) correlates with the strengthening of the Cu–N_{amine} bond. Furthermore, a correlation between the widening of the N_{gua}–Cu–X bond angle and the decrease in the Cu– N_{gua} and Cu–X distances can be observed. The Cu^I atoms in **C3** and **C6** exhibit an approximately Y-shaped geometry, with N_{gua}–Cu–X angles of 147.6(1) (**C3**) and 143.0(1)° (**C6**). In contrast to this, the Cu^I atoms in **C1** and **C4** have an approximately T-shaped coordination geometry, which is indicated by the shorter Cu–X ($X^- = Cl^-$) and Cu–N_{gua} bonds and the resulting widening of the N_{gua}–Cu–X angle. In **C1**, the Cu–N_{amine} donation is already so weak that there is only a Cu–N_{amine} contact [2.639(1) Å], which can also be described as a [2+1] coordination; in **C4** this contact can be described as a very weak bond [2.311(1) Å]. The chlorido complexes (**C1** and **C4**), which are approximately T-shaped, and the iodido complexes (**C3** and **C6**), which are approximately Y-shaped, represent two specific extremes of the trigonal-planar coordination geometry. The coordination geometries of the bromido complexes (**C2** and **C5**) reside between these extremes. Furthermore, in **C1**–**C6**, a torsion of the $N_{amine,gua}C_3$ plane vs. the $C_{gua}N_3$ plane and a torsion of the $C_{gua}N_3$ plane vs. the CuN_2 plane is observed, which minimises the steric interactions of the guanidine unit. The torsion of the $N_{amine,gua}C_3$ vs. the $C_{gua}N_3$ plane in **C4**–**C6**

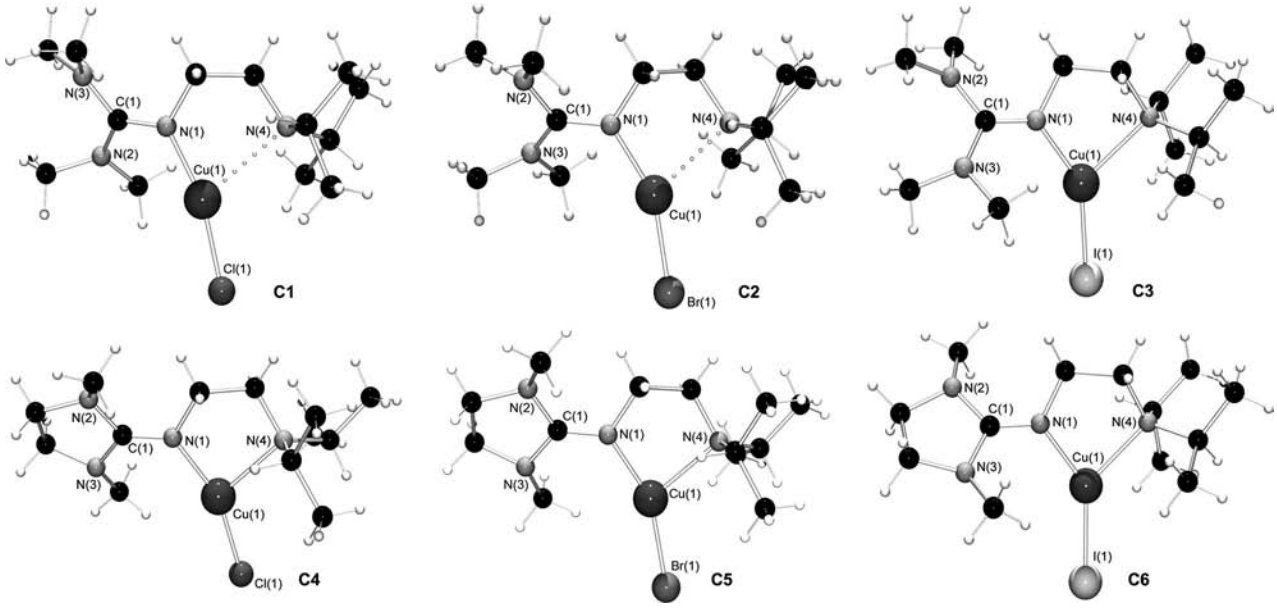

Figure 1. Molecular structures of the complexes **C1** to **C6**.

Table 1. Selected bond lengths [Å] and angles [°] of **C1**–**C6**.

	C1	C2	C3	C4	C5	C6
Cu–X	2.129(1)	2.268(1)	2.441(1)	2.145(1)	2.275(1)	2.459(1)
Cu–N(1)	1.906(1)	1.924(2)	1.945(2)	1.937(1)	1.950(2)	1.982(1)
Cu–N(4)	2.639(1)	2.460(2)	2.332(2)	2.311(1)	2.267(2)	2.233(1)
C(1)–N(1)	1.323(2)	1.311(2)	1.311(3)	1.305(3)	1.301(3)	1.296(2)
C(1)–N(2)	1.357(2)	1.364(2)	1.364(3)	1.377(3)	1.375(3)	1.380(2)
C(1)–N(3)	1.369(2)	1.357(3)	1.359(3)	1.363(3)	1.378(3)	1.379(2)
N–Cu–N	79.1(1)	81.9(1)	84.2(1)	84.5(1)	85.2(1)	85.6(1)
N(1)–Cu–X	164.9(1)	156.0(1)	147.6(1)	158.9(1)	155.8(1)	143.0(1)
N(4)–Cu–X	115.9(1)	122.1(1)	128.1(1)	116.3(1)	118.7(1)	130.8(1)
ρ[22]	0.971	0.964	0.963	0.953	0.945	0.939
$\angle(C_{gua}N_3,CuN_2)$	45.1	42.0	40.5	18.5	19.3	33.9
$\angle(N_{amine,gua}C_3,C_{gua}N_3)$	32.7(av.)	33.4(av.)	34.4(av.)	16.3(av.)	15.9(av.)	15.0(av.)

(16.3 **C4**, 15.9 **C5**, 15.0° **C6**) relative to the torsion in **C1**–**C3** (32.7 **C1**, 33.4 **C2**, 34.4° **C3**) is significantly restricted, because of the rigid ethylene bridge between the two amine functions in **L2**. The torsion of the $C_{gua}N_3$ plane vs. the CuN_2 plane is 18.5–45.1°. It is remarkable that this torsion in TMG complexes is larger than in DMEG complexes.

The C_{gua}=N_{gua} bond lengths in **C1**–**C6** [1.323(2) **C1**, 1.311(2) **C2**, 1.311(3) **C3**, 1.305(3) **C4**, 1.301(3) **C5**, 1.296(2) Å **C6**] are shorter than the C_{gua}–$N_{amine,gua}$ bond lengths [1.363 (av.) **C1**, 1.361 (av.) **C2**, 1.362 (av.) **C3**, 1.370 (av.) **C4**, 1.377 (av.) **C5**, 1.380 Å(av.) **C6**], which indicates a strong double bond character within the guanidine. This is confirmed by the structural parameter ρ, which describes the charge delocalisation within the guanidine function.[22,23] The values were calculated to be 0.971 (**C1**), 0.964 (**C2**), 0.963 (**C3**), 0.953 (**C4**), 0.945 (**C5**) and 0.939 (**C6**). As the ρ values are relatively low, the charge delocalisation can be described as moderate.

Comparison of the herein reported complexes with two further guanidine–amine hybrid ligand complexes of the distorted trigonal-planar coordination type [Cu(TMGdmap)I] (**C7**)[8d] and [Cu(DMEGdmae)I] (**C8**)[24] (Scheme 6) offers the explanation of donor abilities of the guanidine and amine groups. In complex **C7**, the Cu–I and Cu–N_{gua} bond lengths [2.476(1), 1.961(2) Å] are similar to those in **C3** [2.441(1), 1.945(2) Å], which indicates that the donor ability of the TMG guanidine moiety is not affected by the amine group of the ligand. This finding is also observed for the DMEG guanidine moiety, when **C6** is compared to **C8**. The N–Cu–N bite angles of **C6** [85.6(1)°] and **C8** [86.4(1)°] also agree well. In contrast, **C7** [104.2(1)°] exhibits a wider N–Cu–N bite angle than **C3** [84.2(1)°] because of the propylene spacer in **C7**.

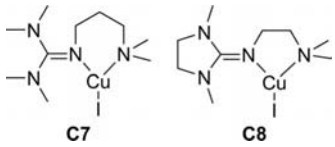

Scheme 6. Comparable mononuclear copper(I) complexes (**C7** and **C8**) with the guanidine hybrid ligands TMGdmap (in **C7**)[8d] and DMEGdmae (in **C8**).[24]

The variation of the amine group, from dimethylamine in **C7** and **C8** to diisopropylamine in reported complexes, has a huge influence on the coordination characteristics of the ligands. Whereas the donor ability of the amine group in **C7** and **C8** is moderately strong with bond lengths of 2.119(2) Å (**C7**) and 2.171(2) Å (**C8**), the donor ability of diisopropylamine in **L1** and **L2** is apparently weaker with bond lengths varying from 2.639(1) to 2.233(1) Å.

These differences in Cu–N_{amine} bond lengths are caused by the sterically demanding isopropyl substituents in **C3** and **C6**, which leads to a widening of the R–N_{amine}–R angle of up to 114.2(1) in **C3** and 114.1(1)° in **C6** [compared to 108.4(2) **C7**, 110.1(2)° **C8**]. This angle widening causes a trigonal-planar distortion of the N environment, which leads to an increase in the s character of the lone pair at the sp^3 hybridised N_{amine} atom. Because of the resulting decrease in the p contribution to the formal sp^3 hybrid, the σ-donor character of the N_{amine} atom decreases and leads to a weakening of the Cu–N_{amine} bond strength.

In addition to the above-described copper(I) complexes, we were able to obtain the crystal structure of one copper(II) complex (**C11**, Figure 2). Like its Cu^I counterpart, **C11** crystallises in the same crystal system and space group. Selected bond lengths and angles for this complex are given in Table 2. The geometry lies between tetrahedral and square planar. Relative to the corresponding Cu^I complex, no significant differences in the bond lengths are observed, with the exception of the Cu(1)–N(4) bond length, which is shorter in **C11** than in **C4** (2.311 Å).

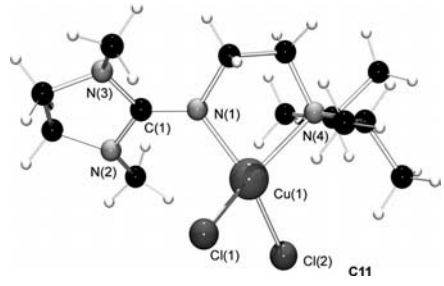

Figure 2. Molecular structure of the complex **C11**.

Table 2. Selected bond lengths [Å] and angles [°] of **C11** and **C9*–C12***.[a]

	C9*	C10*	C11	C11*	C12*
Cu–X	2.170, 2.223	2.342, 2.426	2.225(1), 2.253(1)	2.278, 2.192	2.340, 2.434
Cu–N(1)	1.982	1.972	1.930(3)	1.988	1.998
Cu–N(4)	2.559	2.385	2.121(3)	2.351	2.356
C(1)–N(1)	1.323	1.324	1.295(5)	1.313	1.314
C(1)–N(2)	1.378	1.367	1.369(5)	1.375	1.375
C(1)–N(3)	1.385	1.379	1.370(4)	1.406	1.407
N–Cu–N	80.2	83.0	85.0(1)	84.1	84.2
N(1)–Cu–X	106.9, 110.1	94.5, 144.0	94.5(1), 149.5(1)	98.3, 144.5	99.6, 144.9
N(4)–Cu–X	96.2, 113.1	106.0, 129.0	139.6(1), 101.2(1)	106.7, 109.0	107.2, 110.6
ρ[22]	0.958	0.964	0.946	0.944	0.945
$\angle(C_{gua}N_3,CuN_2)$	25.3	45.0	44.1	8.8	9.2
$\angle(N_{amine,gua}C_3,C_{gua}N_3)$	38.2	36.3	15.4(av.)	15.6	15.6

[a] Theoretical structures are marked with an asterisk.

Density Functional Theory Study

The unique combination of very strong and very weak N donors results in a special coordination situation, which prompted us to study this by DFT methods and NBO analysis. Furthermore, we tried to evaluate the structures of potential bis(chelate) complexes with these ligands. In ATRP, bis(chelate) copper complexes are typically regarded as the active species.[6] All calculated complexes are schematically summarised in Scheme 7, their molecular structures are depicted in the Supporting Information.

The validation of the structural description with Gaussian03 and a standard basis set and functional leads to unsatisfactory results (see Table S1). The amine copper bond length is dramatically underestimated, whereas the guanidine copper bond is predicted to be only slightly too short. This methodology completely fails in the description of the copper coordination, although in other cases, it could be shown that copper complexes can be predicted adequately with the B3LYP/6-31G(d) combination.[2c,8d]

Hence, we chose the combination of the pure functional BP86[25] and def2-TZVP basis set[26] as implemented in Turbomole[27] for the following study. As it is summarised in Table 3, this methodology is better suited to describe the series of complexes. The copper coordination matches considerably better to the real solid-state structures. The copper–halide and copper–guanidine bonds are predicted well, whereas the length of the copper-amine interactions is overestimated relative to the experimental values [e.g. in **C1**: the Cu(1)–N(4) bond is predicted to be 0.12 Å too long]. Remarkably, the deviation between experimental and theoretical structures appears to be distinct only in the critical Cu–N_{amine} interaction.

Table 3. Key geometric parameters of **C1*–C6*** (BP86/def2-TZVP).

	C1*	C2*	C3*	C4*	C5*	C6*
Cu–X	2.122	2.268	2.442	2.133	2.277	2.454
Cu–N(1)	1.914	1.927	1.943	1.933	1.949	1.969
Cu–N(4)	2.755	2.645	2.608	2.561	2.489	2.434
C(1)–N(1)	1.320	1.319	1.319	1.311	1.310	1.310
C(1)–N(2)	1.379	1.378	1.385	1.383	1.402	1.382
C(1)–N(3)	1.385	1.385	1.377	1.402	1.382	1.402
N–Cu–N	77.8	79.5	79.7	81.5	82.8	83.1
N(1)–Cu–X	166.9	162.3	156.4	162.7	158.0	154.0
N(4)–Cu–X	115.3	118.2	123.8	115.8	119.2	122.5

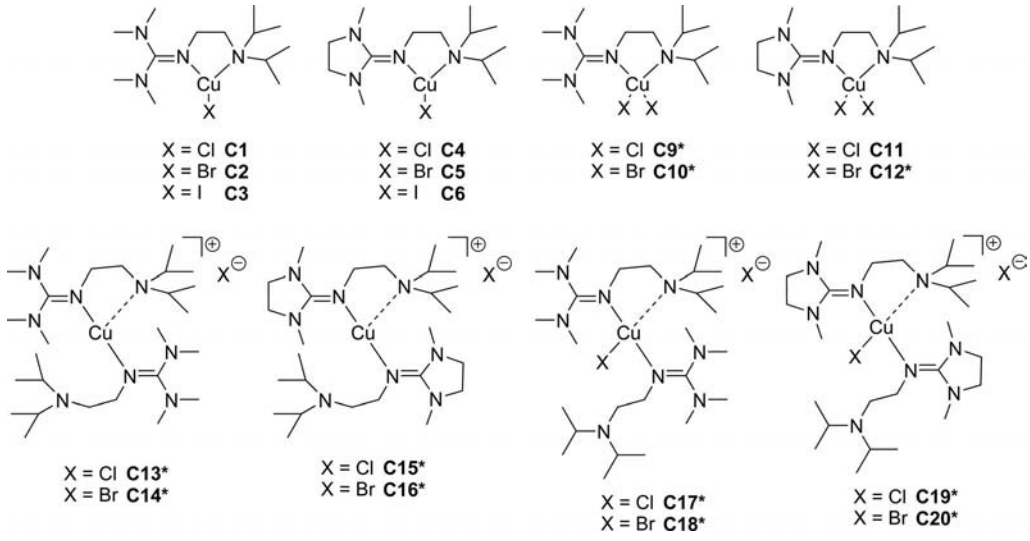

Scheme 7. Overview of molecular and theoretical structures. Theoretical structures are marked with an asterisk.

Table 4. Theoretical structures of the cationic units of the Cu^{I} and Cu^{II} bis(chelate) complexes **C13*–C20***.

	C13*/C14*	C15*/16*	C17*	C18*	C19*	C20*
Cu–X	–	–	2.309	2.468	2.279	2.421
$Cu–N_{gua}$	1.917, 1.917	1.926, 1.930	1.998, 2.006	1.994, 1.999	1.968, 2.025	1.950, 1.993
$Cu–N_{amine}$	2.825	2.697	2.378	2.423	3.016	3.310
$C_{gua}–N(1)$	1.330, 1.330	1.320, 1.320	1.331, 1.347	1.331, 1.349	1.332, 1.321	1.334, 1.322
$C_{gua}–N(2)$	1.371, 1377	1.380, 1.384	1.369, 1.373	1.370, 1.374	1.374, 1.374	1.372, 1.373
$C_{gua}–N(3)$	1.374, 1.377	1.382, 1.383	1.359, 1.375	1.359, 1.375	1.378, 1.382	1.379, 1.382
$N_{gua}–Cu–N_{gua}$	170.7	175.1	158.5	159.3	148.9	147.8
$N_{gua}–Cu–N_{amine}$	77.2, 110.9	78.7, 106.1	81.4, 106.7	81.0, 106.5	72.6, 100.0	68.6, 99.5
$N_{gua}–Cu–X$	–	–	92.0, 100.9	92.0, 100.6	102.7, 108.0	105.1, 107.0

The special challenge lies in the description of the coordinative environment in the bis(chelate) complexes **C13*–C20*** (Table 4). Two guanidine-isopropylamine ligands and one halogen atom cause enormous steric encumbrance, and the complexes tend to drive the weaker amine donor function out. In the case of **L1**, this results in a coordination mode where one **L1** binds in a bidentate fashion and one **L1** binds only with the guanidine function (see Supporting Information for structures **C13*–C20***), whereas for copper(II) complexes with **L2**, both amine groups tend to be driven out. Hence, the resulting complex geometries have only a limited explanatory power.

For additional insight into the bonding situation in **C1–C6**, we performed natural bond order (NBO) calculations with BP86/def2-TZVP in Gaussian03. These calculations allow the dissection of the influence of the guanidine ligand and halide on copper coordination. The tetramethylguanidine (TMG) group is a significantly stronger donor relative to the dimethylethyleneguanidine (DMEG) group, which results in the shorter $Cu–N_{gua}$ bond lengths in complexes **C1–C3** in the experimental and calculated data. In return, the amine donor binds more weakly in these complexes as the copper is coordinatively satisfied with the guanidine and the halide donors, which results in a [2+1] coordination. This coordination motif is more strongly developed in the chlorido complexes. In the DMEG-containing complexes **C4–C6**, the slightly weaker guanidine donation is compensated by a stronger amine donation. This is reflected in the energies of the charge transfer between amine and copper (Table 5), which are significantly higher for the DMEG complexes. The influence of the halide is present for this bonding aspect, too. As iodine is a slightly weaker donor, the amines donate marginally more in the iodido complexes. Remarkably, the charge transfer within the guanidine moiety depends on the substitution pattern: in DMEG complexes, the lone pairs of the N_{amine} atoms within the guanidine unit donate more strongly into the antibonding C=N orbital than that in the TMG complexes. This is valid for the uncoordinating ligands as well (TMGd^{i}pae: 23.26, 27.29 kcal/mol, DMEGd^{i}pae: 30.79, 33.34 kcal/mol) and correlates with the intraguanidine torsion, which is higher for TMG systems (around 33°) than for DMEG systems (approx. 10°, vide supra).[8c,19b,13f,13g]

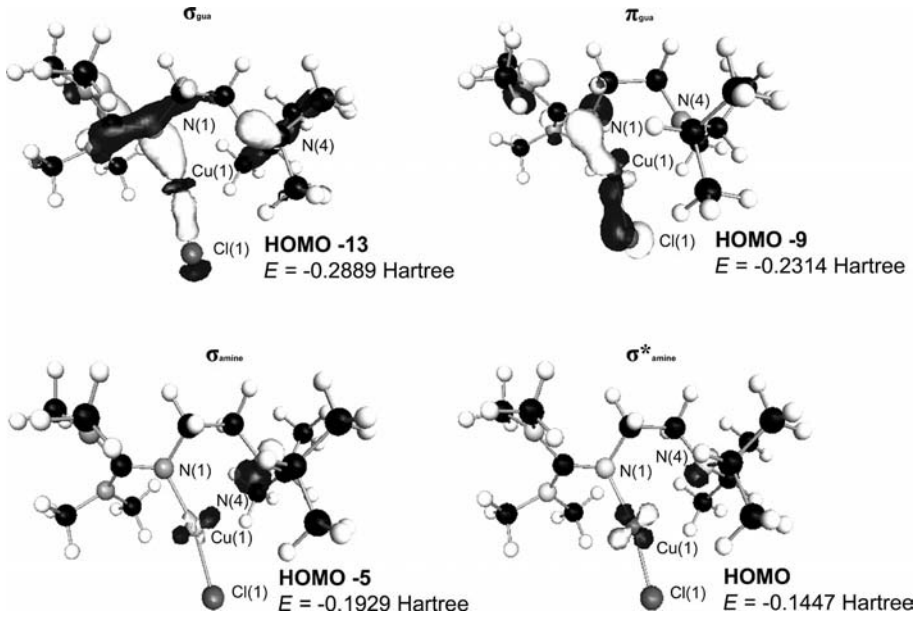

Figure 3. Selected orbitals of the complex [Cu(TMGd^{i}pae)Cl] (**C1**) obtained by DFT analysis.

Table 5. NBO analysis of intramolecular charge-transfer interactions (BP86/def2-TZVP, energies in kcal/mol).[a]

	C1*	C2*	C3*	C4*	C5*	C6*
LP[N(4)] → Cu	3.3	5.1	6.0	6.1	8.3	11.7
Cu–N_{gua} → BD*$_{gua}$	13.1	13.1	13.0	15.5	15.4	15.6
LP[N(2,3)] → BD*$_{gua}$	39.8	39.4	40.5	45.6	45.9	46.9
	39.5	39.8	41.8	56.6	56.8	58.6

[a] LP: lone pair, BD*: antibonding orbital.

A possible reason for the weak copper amine bond lies in the orbital structure of these complexes. Figure 3 depicts the most characteristic orbitals, namely those involving the σ guanidine–copper bond, the π guanidine–copper bond and the σ amine–copper interaction, together with the σ* amine–copper interaction. The last one represents the HOMO of the complex and thus weakens the amine–copper interaction. The σ donation from guanidine to copper is the most dominant interaction. Backbonding from copper to guanidine occurs through a charge transfer from the Cu–N_{gua} σ bonding orbital to the C=N_{gua} antibonding orbital (Table 5). A comparison between **C1*** and **C4*** shows that the orbital energies change slightly: in **C4***, the σ_{gua} orbital lies at –0.2881 Hartree at a similar position, whereas the π_{gua} orbital is lifted to –0.2229 Hartree. The bonding σ_{amine} orbital is lowered to –0.201 Hartree, and the antibonding σ^*_{amine} orbital is lifted to –0.1401 Hartree. This explains why the Cu–N_{amine} interaction in the DMEG complexes is stronger.

For ATRP application, the ability to accept or lose a halogen atom, which is discussed as halogen bond dissociation energy (BDE), is of great importance. Table 6 summarises the estimation for the BDE of complexes **C9***–**C12*** and **C17***–**C20***. Because of the problematic geometry optimisation of the bis(chelate) complexes, the resulting energies are error-prone such that they can only serve as a rough estimation. For this reason, only electronic energy differences are reported. All BDEs lie in the range 33–45 kcal/mol. **C18*** has the smallest BDE, which allows the prediction that the corresponding copper(I) complex, **C14***, should be a good ATRP catalyst.

Table 6. Calculated bond dissociation energies (BP86/def2-TZVP).

	BDE [kcal/mol]
C9*	40.9
C10*	39.0
C11*	45.4
C12*	37.1
C17*	43.0
C18*	33.6
C19*	40.8
C20*	41.8

Copper-Mediated Atom Transfer Radical Polymerisation with L1 and L2 as Ligands

Bisguanidines and their derivatives bis(imidazolin-2-imines) promote a moderately controlled ATRP of styrene with high polydispersities.[19] Our aim was to investigate the ligands, which combine a guanidine moiety as a strong donor and an amine donor (similar to the TMEDA ligand), in order to determine the influence of steric encumbrance at the copper atom. For the estimation of the catalytic activity, we performed styrene ATRP with both ligands (**L1**, **L2**) combined with CuCl and CuBr. The catalytic system is generated in situ with 2 equiv. of the ligand. This ratio of 2:1 for the transition metal to the bidentate ligand is known in the literature to promote the most-efficient ATRP.[28,29] 1-Chlorophenylethane (1-PECl) and 1-bromophenylethane (1-PEBr) were used as initiators. The catalyst and initiator to styrene ratio was 1:100. Polymerisation was performed in bulk and in solution with acetonitrile as solvent at reaction temperatures between 70 to 130 °C.

As a basic study of ATRP activity, we performed polymerisation in bulk at different temperatures with both ligands. Table 7 summarises the results of bulk polymerisation performed at 70 and 110 °C. Polymerisation with **L1** and CuCl performed at 70 and 110 °C shows the same characteristics, indicating an uncontrolled ATRP, with higher molecular weights and broad molecular weight distributions, which in controlled radical polymerisation lie between 1.0 and 1.5. Polymerisation at lower temperatures results as expected in a less controlled manner compared to polymerisation at higher temperatures. Consequently further polymerisations were performed at 110 °C. The catalytic system 2**L1**/CuBr provides a fast ATRP and shows consistent obtained molecular weight with calculated molecular weight as the first indication for controlled radical polymerisation. The polydispersity of 1.64 is still relatively high, but closer to 1.5, which is the upper limit for a well-controlled ATRP process.[6]

Table 7. Bulk polymerisation with 2**L1**/CuCl (**C13***), 2**L1**/CuBr (**C14***), 2**L2**/CuCl (**C15***) and 2**L2**/CuBr (**C16***) as catalyst and 1-PECl as initiator for polymerisation with **C13***/**C15*** and 1-PEBr, with **C14***/**C16***.[a]

Catalyst	T [°C]	t [h]	Yield [%]	$M_{n,calcd.}$ [g/mol][b]	M_n [g/mol]	M_w/M_n
C13*	70	24	12	1248	57000	1.83
C13*	110	24	97.6	10150	21500	1.79
C14*	110	3.5	>98	10400	10350	1.64
C15*	110	4.5	56.2	5845	41300	1.57
C16*	110	3.5	93.3	9700	11870	1.93

[a] Reaction conditions: $[Styrene]_0/[\mathbf{C13^*}$ or $\mathbf{C15^*}]_0/[1\text{-PECl}]_0$ = 100:1:1, $[Styrene]_0/[\mathbf{C14^*}$ or $\mathbf{C16^*}]_0/[1\text{-PEBr}]_0$ = 100:1:1. [b] Calculated with the equation $M_{n,calcd.} = [M]_0/[I]_0 \times M_M \times Y$, where $[M]_0/[I]_0$ is the ratio of monomer-to-initiator starting concentration, M_M the molecular weight of monomer and Y the yield.

ATRP experiments performed with the catalytic systems 2**L2**/CuCl and 2**L2**/CuBr at 110 °C are in contrast to each other because the system with CuCl shows bad control over molecular weight but a relatively narrow weight distribution, whereas with CuBr the reverse is observed with relatively good agreement between obtained and calculated molecular weights, but with high polydispersity.

Comparison of bulk ATRP with **L1** and **L2** exhibits that **L1** is the better ligand for further application in ATRP. As described in the literature,[6] our study also shows the effi-

ciency of copper bromide relative to copper chloride.[6,16] Finally, the catalytic system 2**L1**/CuBr shows the highest potential for application in ATRP.

Remarkable for all applied catalytic systems was the good solubility in styrene, which results in a homogeneous ATRP already at the beginning of the polymerisation process.

To evidence the controlled/living character of styrene polymerisation with our catalytic system, we performed kinetic studies with 2**L1**/CuBr (named as **C14***). The kinetic plots are presented in Figures 4 and 5. The semilogarithmic plot of $\ln([M]_0/[M])$ vs. time shows the typical linearity for a controlled process until a polymerisation time of 100 min, after which a clear deviation to higher conversion is observed. The molecular weights (M_n) increase linearly with conversion and do not deviate from the theoretical molecular weights ($M_{n,calcd.}$), which points to a controlled process. The polydispersity decreases to a value of 1.31 at a conversion of 70% and increases after this to a value of 1.66. This course for the polydispersity is in accordance with the semilogarithmic plot of $\ln([M]_0/[M])$ vs. time, which deviates from linearity after 100 min. Overall, the kinetic plots show evidence for a well-controlled radical polymerisation process until a conversion of 70% and a polymerisation time of 100 min, after which a loss of polymerisation control is observed. This trend in styrene ATRP was observed by Matyjaszewski earlier with the bidentate amine ligand TMEDA; the loss of control after a certain polymerisation time could be explained by the decrease in deactivator concentration because of its low solubility.[28]

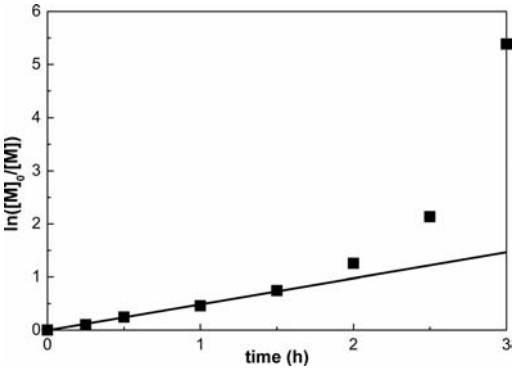

Figure 4. Kinetic plot for the bulk ATRP of styrene using **C14***. Conditions: 110 °C; $[styrene]_0$ = 11 M; $[1\text{-PEBr}]_0 = [CuBr]_0 = [\mathbf{L1}]_0/2$ = 0.01 M.

As control experiment, we performed kinetics with the 2:1 complex generated from 1 equiv. **C2** and one additional equivalent of **L1** under the same conditions. The resulting kinetics (see Figures S1 and S2 in the Supporting Information) does not show significant differences, which leads to the conclusion that, in both cases, the same catalytic species is generated in the polymerisation environment. Further, we investigated the activity of the synthesised 1:1 complex **C2**, where we expected a low activity according to the literature.[6] Though we observed a marginal lower polymerisation rate than with the 2:1 in situ catalyst, the kinetics show the same phenomenology (Figures 6 and 7). Good polymerisation control is observed until a polymerisation time of 2.5 h, the polydispersity decreases until a value of 1.2, followed by an increase. This relatively high polymerisation control was not expected and not described in the literature before. Possible explanations can be provided by the DFT considerations made above: the mono(chelate) complexes possess a stable coordination sphere, whereas the bis(chelate) complexes suffer from weak coordination of the amine group. In the DFT, the bis(chelate) complexes tend to drive out the amine groups, which results in monodentate coordination of the guanidine ligands. This unstable coordination hinders the formal "bis(chelate)" complexes from being perfect ATRP catalysts. In contrast to this, the mono(chelate) complexes appear to be surprisingly good catalysts as they easily transfer halogen atoms, which has been supported by the BDE calculations.

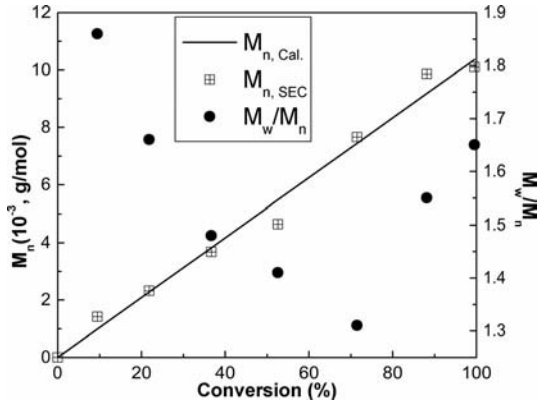

Figure 5. Dependence of molecular weight, M_n, and molecular weight distribution, M_w/M_n, on monomer conversion for styrene ATRP with **C14***. Conditions: 110 °C; $[styrene]_0$ = 11 M; $[1\text{-PEBr}]_0 = [CuBr]_0 = [\mathbf{L1}]_0/2$ = 0.01 M.

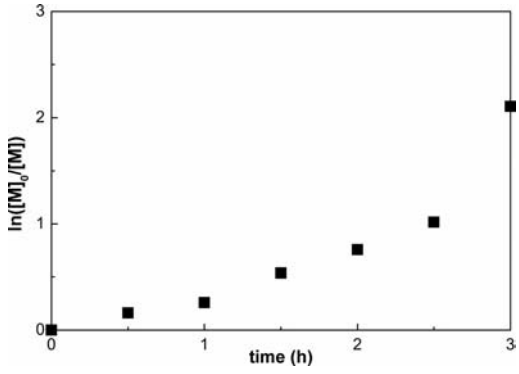

Figure 6. Kinetic plot for the bulk ATRP of styrene using **C2**. Conditions: 110 °C; $[styrene]_0$ = 11 M; $[1\text{-PEBr}]_0 = [\mathbf{C2}]_0$ = 0.01 M.

In addition to bulk polymerisation, we performed ATRP in solution to see how it influences the polymerisation; we therefore chose acetonitrile because it dissolves guanidine copper complexes best. As was reported by Matyjaszewski et al., additives only influence the ATRP process if they have coordinating groups.[30] We performed the polymerisa-

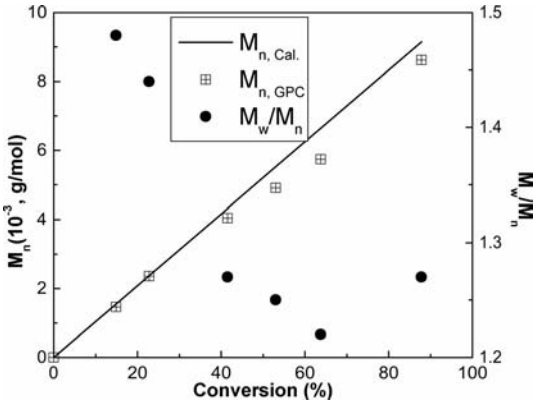

Figure 7. Dependence of molecular weight, M_n, and molecular weight distribution, M_w/M_n, on monomer conversion for styrene ATRP with **C2**. Conditions: 110 °C; $[styrene]_0$ = 11 M; $[1\text{-PEBr}]_0$ = $[\mathbf{C2}]_0$ = 0.01 M.

tion experiments with 50% acetonitrile (v/v according to styrene volume) at different temperatures (Table 8). The styrene/initiator/catalyst ratio was as in the bulk polymerisation 100:1:1, and 1-PECl and 1-PEBr were used as initiators. Polymerisation in solution is slower than bulk polymerisation because of the lower concentration of styrene. We found that the molecular weights and polydispersities do not differ from those for the bulk polymerisation. In solution, the promoted ATRP has a bad control with a far too high molecular weight and polydispersity with the catalytic system **C13*** at all tested temperatures. In good agreement with bulk polymerisation, polymerisation in solution at 110 °C with **C14*** results in a relatively good agreement between the measured and calculated molecular weights and in a polydispersity near the desired range. In contrast, polymerisation at 130 °C with **C14*** shows a decrease in polymerisation control, as pointed out by a broad molecular weight distribution.

Polymerisation with **L1** (TMG unit) shows a higher activity for ATRP than that with **L2** with DMEG. This observation correlates with the higher donor ability of the TMG donors observed in the solid-state and predicted by gas-phase DFT. Although the ligand **L1** has two relatively huge donor atoms, the activity in ATRP is comparable to that with the bidentate aliphatic ligand TMEDA. The fact that the strong N donor of the guanidine moiety does not offer an enhancement in ATRP in comparison to the weaker-donating TMEDA can be related to the very weakly donating diisopropylamine.

Overall, the phenomenology of styrene kinetics with **L1** relative to that with TMEDA shows the same trend, e.g. good control until a conversion of 70%, linearity of molecular weight with conversion and increase in polydispersity after an initial decrease to the value of 1.3. In addition to the similar degree of control, our system mediates a much faster polymerisation. This feature and the fact that the catalytic system is very soluble in styrene make the guanidine hybrid ligands competitive ligands for the application in ATRP. Surprisingly, polymerisation with the 1:1 complex **C2** also proceeds in a controlled manner until 70% and shows the same kinetic phenomenology as that with the 2:1 complex **C14***. This unexpected result opens up the way to further studies on bidentate mono(chelate) copper complexes for ATRP.

Conclusions

With the synthesised ligands **L1** and **L2**, we obtained the copper chlorido, bromido and iodido complexes. Comparison of complexes with **L1** and **L2** show a significant difference in the donor ability of the guanidine moiety TMG and DMEG: TMG is the stronger donor. The amine group always shows a weak coordination to copper. In the two halide series, the same trends with regard to coordination geometry and contraction of the $Cu–N_{amine}$ bond as a function of the halide is observed. The coordination can be described as [2+1], with a T-shaped geometry in chlorido complexes and a Y-shaped geometry in iodido complexes; the bromido complexes reside between the two geometries. The variation in geometry towards the Y-shape geometry is consistent with a contraction of the $Cu–N_{amine}$ bond. DFT calculations allow the dissection of the influence of guanidine ligand and halide on copper coordination, reflecting the compensation of the slightly weaker guanidine donation of DMEG (**C4**–**C6**) with a stronger amine donation in the complexes by the energies of the charge transfer between amine and copper, which are significantly higher for the DMEG complexes. NBO analysis explains the weakness of the amine bond by relation to the occupation of the σ* orbital of the $Cu–N_{amine}$ bond. The σ donation of guanidine to copper is the most-dominant binding interaction, and

Table 8. Polymerisation with 2**L1**/CuCl (**C13***) and 2**L1**/CuBr (**C14***) as catalyst and 1-PECl as initiator for polymerisation with **C13*** and 1-PEBr with **C14*** at temperatures 70, 110 and 130 °C with 50% (v/v) acetonitrile as solvent.[a]

Catalyst	T [°C]	t [h]	Yield [%]	$M_{n,calcd.}$ [g/mol][b]	M_n [g/mol]	M_w/M_n
C13*	70	4	10	1042	60000	1.70
C13*	110	4	56	5832	40000	1.72
C13*	130	2	91	9478	22000	1.68
C14*	110	4	92	9582	10500	1.63
C14*	130	4	92	9582	10500	2.00

[a] Reaction conditions: $[Styrene]_0/[\mathbf{C13*}]_0/[1\text{-PECl}]_0$ = 100:1:1, $[Styrene]_0/[\mathbf{C14*}]_0/[1\text{-PEBr}]_0$ = 100:1:1. [b] Calculated with the equation $M_{n,calcd.} = [M]_0/[I]_0 \times M_M \times Y$, where $[M]_0/[I]_0$ is the ratio of monomer-to-initiator starting concentration, M_M the molecular weight of monomer and Y the yield.

backbonding from copper to the guanidine occurs through a charge transfer from the Cu–N σ bonding orbital to the C=N antibonding orbital.

ATRP with **L1** and **L2** as ligands shows, at first sight, a less-controlled polymerisation, but kinetic studies performed with the best system (2**L1**/CuBr) evidence the controlled/living character of the polymerisation until a polymerisation time of 100 min, after which a deviation of $\ln([M]_0/[M])$ to higher conversions and an increase in polydispersity occurs. With a high polymerisation rate, good solubility and a competitive behaviour with regard to polymerisation control, our catalytic system with guanidine hybrid ligands shows high potential for application in ATRP.

Experimental Section

General: Ligand syntheses were performed under argon by using standard Schlenk techniques, complexes were prepared in a glove box under nitrogen atmosphere. Solvents were purified according to literature procedures and kept under nitrogen.[31] All chemicals were used as purchased, with the exception of styrene, which was destabilised by eluting through a column of neutral Al_2O_3. The Vilsmeier salts *N*,*N*′-dimethylethylenechloroformamidinium chloride (DMEG) and *N*,*N*,*N*′,*N*′-tetramethylchloroformamidinium chloride (TMG) were synthesised as described in the literature.[21]

Physical Methods: Spectra were recorded with the following spectrometers. NMR: Bruker Avance 500. The signals were calibrated to the residual signals of the deuterated solvent [$\delta_H(CDCl_3)$ = 7.26 ppm]. IR: Nicolet P510. MS (EI, 70 eV): Finnigan MAT 8200. Elemental analyses: Perkin–Elmer analysator type 2400. Measurements of molecular weight distributions of the polymers were performed by gel permeation chromatography (GPC) on a Waters GPC 2000 instrument equipped with a precolumn (10 μm) and a combination of PSS-SDV columns with porosities of 10^5 and 10^3 Å, a HPLC pump (L6200, Merck Hitachi) and a refractive index detector (Smartline RI Detector 2300, Knauer). THF was used as mobile phase at a flow rate of 1 mL min^{-1}. The instrument was calibrated with standard polystyrene samples. Sample concentrations were 2–3 g L^{-1}.

X-ray Analyses: Crystal data for **C1**–**C6** are presented in Table 9. Data for **C1**–**C3** and **C6** were collected on a Bruker-AXS SMART[32] APEX CCD diffractometer with Mo-K_α radiation (λ = 0.71073 Å) and a graphite monochromator. Data reduction and absorption correction were performed with the programs SAINT and SADABS.[32] The structures were solved by direct and conventional Fourier methods, and all non-hydrogen atoms were refined anisotropically by full-matrix least-square techniques based on F^2 (SHELXTL[33]). Hydrogen atoms were derived from difference Fourier maps and placed at idealised positions, riding on their parent C atoms, with isotropic displacement parameters $U_{iso}(H)$ = $1.2U_{eq}(C)$ and $1.5U_{eq}$ – (C_{methyl}). All methyl groups were allowed to rotate but not to tip.

Data for complexes **C4**, **C5** and **C11** were collected with a Xcalibur S Diffractometer from Oxford Diffraction with graphite-monochromated Mo-K_α radiation (λ = 0.71073 Å). The data collection covered almost the whole sphere of reciprocal space with eight sets at different κ angles and 430 frames through ω rotation (Δ/ω = 1°) at two times 60 s per frame. The crystal-to-detector distance was 4.5 cm. Crystal decay was monitored by repeating the initial frames at the end of data collection. Analysis of the duplicate reflections showed that there was no indication of any decay. The structure was solved by direct methods and successive difference Fourier syntheses. Refinement applied full-matrix least-squares methods. The hydrogen atoms were placed in geometrically calculated positions by using a riding model with U_{iso} constrained 1.2 times U_{eq} for the carrier atom.

Full crystallographic data (excluding structure factors) for **L4** and **L6** have been deposited with the Cambridge Crystallographic Data Centre as supplementary no. CCDC-796504 (for **C1**), -796505 (for **C2**) and -796506 (for **C3**), -799099 (for **C4**), -796702 (for **C5**), -796507 (for **C6**) and -812975 (for **C11**) contain the supplementary crystallographic data for this paper. These data can be obtained free of charge from The Cambridge Crystallographic Data Centre via www.ccdc.cam.ac.uk/data_request/cif.

Computational Details: Density functional theory (DFT) calculations were performed with the programs Gaussian 03[34] and Turbomole.[27] The geometries of the complexes and ligands were optimised (Table S1, Table 2) by using the B3LYP[33] hybrid DFT functional and the 6-31 g(d) basis sets implemented in Gaussian on all atoms or the pure functional BP86[25] and def2-TZVP basis set.[26] The starting geometries of complexes **C1**–**C6** were generated from their crystal structures. NBO analysis was performed with NBO 3.1 as implemented in Gaussian03.[35] BDE calculations were performed following the method described elsewhere.[36]

General Procedure for the Synthesis of Hybrid Ligands: To a solution of 2-(diisopropylamino)ethylamine (40 mmol) and triethylamine (40 mmol) in dry MeCN (40 mL) was added dropwise under vigorous stirring and ice cooling a solution of the chloroformamidinium chloride (40 mmol) in dry MeCN (40 mL). After 3 h at reflux, aqueous NaOH (40 mmol, 1.6 g, 10 mL) was added. MeCN and the resulting triethylamine were removed under vacuum, and for the deprotonation of the formed guanidine hydrochloride 50% KOH solution (10 mL) was added to the residue. Finally, the free base was extracted into MeCN (3 × 30 mL). The organic phase was dried under Na_2SO_4, and, after filtration, the solvent was evaporated under reduced pressure.

2-[2-(Diisopropylamino)ethyl]-1,1,3,3-tetramethylguanidine (TMGd^{i}pae, L1): Orange oil. Yield: 8.34 g (86%). ^{1}H NMR (500 MHz, $CDCl_3$, 298 K): δ = 0.95 (s, 6 H, CH_3), 0.97 (s, 6 H, CH_3), 2.45–2.48 (m, 2 H, CH_2), 2.59 (s, 6 H, CH_3), 2.68 (s, 6 H, CH_3), 2.91–2.99 (m, 2 H, CH), 3.05–3.09 (m, 2 H, CH_2) ppm. ^{13}C NMR (125 MHz, $CDCl_3$, 298 K): δ = 20.7 (CH_3), 38.7 (CH_3), 39.6 (CH_3), 48.7 (CH_2), 49.2 (CH), 52.2 (CH_2), 160.1 (C_{gua}) ppm. EI-MS: *m*/*z* (%) = 242.3 (26) [M^+], 199 (83) [M^+ – $CH(CH_3)_2$], 154 (14), 142 (11) [M^+ – $N\{CH(CH_3)_2\}_2$], 128 (28) [M^+ – $H_2CN\{CH(CH_3)_2\}_2$], 126 (98), 115 (46), 114 (100) [$H_2CN(CH(CH_3)_2)_2^+$], 100 (10), 97 (9), 86 (25), 85 (96), 72 (83), 70 (26), 58 (17), 56 (14), 44 (42) [$N(CH_3)_2^+$], 42 (34). IR (Nujol): $\tilde{\nu}$ = 2964 (vs), 2931 (s), 2870 (s), 2839 (m), 2798 (m), 1624 [vs, ν(C=N)], 1495 (m), 1454 (m), 1361 (vs), 1329 (w), 1292 (w), 1238 (m), 1207 (m), 1174 (m), 1132 (s), 1082 (w), 1062 (m), 1022 (w), 991 (m), 941 (vw), 914 (w) cm^{-1}.

N^1-(1,3-Dimethylimidazolidin-2-yliden)-N^2,N^2-diisopropylethan-1,2-diamine (DMEGd^{i}pae, L2): Orange oil. Yield: 8.19 g (85%). ^{1}H NMR (500 MHz, $CDCl_3$, 298 K): δ = 0.95 (s, 6 H, CH_3), 0.97 (s, 6 H, CH_3), 2.48–2.51 (m, 2 H, CH_2), 2.74 (s, 6 H, CH_3), 2.95 (sep, 2 H, CH), 3.09 (s, 4 H, CH_2), 3.28–3.31 (m, 2 H, CH_2) ppm. ^{13}C NMR (125 MHz, $CDCl_3$, 298 K): δ = 20.7 (CH_3), 20.8 (CH_3), 36.3 (CH_3), 49.2 (CH_2), 49.3 (CH), 49.4 (CH_2), 49.9 (CH_2), 157.3 (C_{gua}) ppm. EI-MS: *m*/*z* (%) = 240.2 (41) [M^+], 198 (16), 197 (75) [M^+ – $CH(CH_3)_2$], 140 (35) [M^+ – $N(CH(CH_3)_2)_2$], 127 (73), 126 (100) [M^+ – $H_2CN(CH(CH_3)_2)_2$], 114 (86) [$H_2CN(CH(CH_3)_2)_2^+$], 98 (10), 85 (20), 72 (52), 70 (21), 56 (46), 44 (16), 43 (19), 42 (20). IR (Nu-

Table 9. Crystal data and structure refinement for complexes **C1**–**C6**.

	C1	C2	C3	C4	C5	C6	C11
Empirical formula	$C_{13}H_{30}ClCuN_4$	$C_{13}H_{30}BrCuN_4$	$C_{13}H_{30}ICuN_4$	$C_{13}H_{28}ClCuN_4$	$C_{13}H_{28}BrCuN_4$	$C_{13}H_{28}ICuN_4$	$C_{13}H_{28}Cl_2CuN_4$
Molecular mass [g mol^{-1}]	341.40	385.86	432.85	339.38	383.84	430.83	374.83
Crystal system	monoclinic	monoclinic	monoclinic	monoclinic	monoclinic	monoclinic	monoclinic
Space group	$P2_1/c$	$P2_1/c$	$P2_1/c$	$P2_1/c$	$P2_1/c$	$C2/c$	$P2_1/c$
a [Å]	15.498(4)	15.6435(18)	15.6554(9)	11.4645(7)	11.6893(6)	29.367(5)	10.2830(12)
b [Å]	7.986(2)	7.9989(9)	8.0491(4)	9.3935(4)	9.4850(4)	8.0062(15)	11.5742(13)
c [Å]	15.217(4)	15.2512(17)	15.6038(8)	15.5812(11)	15.4971(8)	15.451(3)	14.8057(19)
α [°]	90	90	90	90	90	90	90
β [°]	114.253(5)	114.335(2)	113.0440(10)	107.811(7)	107.115(5)	111.163(3)	102.821(12)
γ [°]	90	90	90	90	90	90	90
V [Å^3]	1717.3(7)	1738.8(3)	1809.36(17)	1597.54(16)	1642.12(14)	3387.8(11)	1718.2(4)
Z	4	4	4	4	4	8	4
$D_{calcd.}$ [g cm^{-3}]	1.320	1.474	1.589	1.411	1.553	1.689	1.449
F(000)	728	800	872	720	792	1728	788
Temperature [K]	120(2)	120(2)	120(2)	173(2)	173(2)	120(2)	173(2)
Θ range [°]	1.44–27.87	1.43–27.88	1.41–27.88	2.57–25.50	2.55–25.50	1.49–27.88	2.03–25.50
Reflections collected	14317	13698	16387	11692	11419	14394	11209
Independent reflections	4087	4138	4310	2968	3054	4036	3158
R_1 [$I \geq 2\sigma(I)$]	R_1 = 0.0322, wR_2 = 0.0846	R_1 = 0.0285, wR_2 = 0.0788	R_1 = 0.0225, wR_2 = 0.0550	R_1 = 0.0276, wR_2 = 0.0491	R_1 = 0.0240, wR_2 = 0.0537	R_1 = 0.0179, wR_2 = 0.0461	R_1 = 0.0417, wR_2 = 0.0618

jol): $\tilde{\nu}$ = 2965 (vs), 2933 (s), 2871 (m), 1666 [vs, ν(C=N)], 1537 (m), 1508 (m), 1481 (m), 1464 (m), 1414 (w), 1383 (s), 1361 (m), 1329 (vw), 1281 (m), 1265 (m), 1230 (w), 1205 (m), 1182 (w), 1142 (vw), 1119 (w), 1065 (vw), 1018 (w), 980 (vw), 957 (w) cm^{-1}.

Synthesis of Copper Complexes: To a solution of TMGd^{i}pae or DMEGd^{i}pae (1.0 mmol) in a mixture of dry THF and MeCN (1–2 mL) was added dropwise under vigorous stirring a solution of the copper compound (1.0 mmol, CuI, CuBr and CuCl) in dry MeCN (1–2 mL). From the clear yellow or orange solution, crystals suitable for X-ray diffraction were obtained by slow diffusion of diethyl ether. All complexes crystallise as colourless solids.

[Cu(TMGd^{i}pae)Cl] (C1): Yield: 272 mg (80%). IR (KBr): $\tilde{\nu}$ = 2969 (s), 2944 (s), 2898 (s), 2863 (s), 2838 (m), 2798 (m), 1573 [vs, ν(C=N)], 1531 (vs), 1454 (s), 1425 (vs), 1421 (s), 1394 (vs), 1364 (s), 1319 (w), 1280 (m), 1257 (w), 1236 (s), 1197 (m), 1176 (s), 1149 (s), 1137 (vs), 1122 (s), 1083 (s), 1038 (s), 973 (w), 954 (m), 914 (w), 889 (m), 836 (vw), 775 (w), 686 (w), 595 (w), 578 (w), 538 (vw), 505 (vw), 480 (vw), 420 (vw) cm^{-1}. $C_{13}H_{30}ClCuN_4$ (341.40 g/mol): calcd. C 45.7, H 8.9, N 16.4; found C 45.6, H 8.9, N 16.4.

[Cu(TMGd^{i}pae)Br] (C2): Yield: 320 mg (85%). IR (KBr): $\tilde{\nu}$ = 2971 (s), 2944 (s), 2896 (s), 2863 (s), 2796 (w), 1573 [vs, ν(C=N)], 1529 (vs), 1454 (s), 1425 (s), 1392 (s), 1363 (m), 1276 (w), 1236 (m), 1195 (w), 1172 (m), 1147 (s), 1135 (s), 1081 (s), 1070 (w), 1029 (m), 952 (m), 912 (w), 890 (m), 836 (vw), 775 (w), 686 (w), 595 (w), 538 (vw), 507 (vw), 478 (vw) cm^{-1}. $C_{13}H_{30}BrCuN_4$ (385.9 g/mol): calcd. C 40.5, H 7.8, N 14.5; found C 40.8, H 8.0, N 14.5.

[Cu(TMGd^{i}pae)I] (C3): Yield: 346 mg (80%). EI-MS: m/z (%) = 242 (9) [TMGd^{i}pae$^+$], 199 (96) [TMGd^{i}pae$^+$ – CH(CH$_3$)$_2$], 154 (17), 142 (15) [TMGd^{i}pae$^+$ – N(CH(CH$_3$)$_2$)$_2$], 140 (14), 128 (97) [TMGd^{i}pae$^+$ – H$_2$CN(CH(CH$_3$)$_2$)$_2^+$], 114 (94) [H$_2$CN(CH(CH$_3$)$_2$)$_2^+$], 100 (10), 97 (16), 86 (51), 85 (100), 84 (58), 72 (88), 70 (78), 58 (36), 56 (30), 43 (76) [CH(CH$_3$)$_2^+$]. IR (KBr): $\tilde{\nu}$ = 2992 (m), 2971 (m), 2934 (m), 2899 (m), 2862 (m), 2795 (m), 1572 [vs, ν(C=N)], 1529 (vs), 1482 (m), 1453 (s), 1423 (vs), 1392 (vs), 1363 (m), 1349 (m), 1275 (w), 1254 (w), 1237 (m), 1193 (w), 1169 (m), 1147 (s), 1134 (s), 1125 (s), 1081 (m), 1053 (w), 1030 (m), 967 (w), 951 (w), 913 (w), 892 (w), 877 (w), 836 (vw), 804 (vw), 775 (w), 726 (vw), 687 (w), 600 (w), 580 (vw), 559 (vw), 539 (vw), 510 (vw) cm^{-1}. $C_{13}H_{30}CuIN_4$ (432.8 g/mol): calcd. C 36.1, H 7.0, N 12.9; found C 36.4, H 7.1, N 12.7.

[Cu(DMEGd^{i}pae)Cl] (C4): Yield: 220 mg (65%). IR (KBr): $\tilde{\nu}$ = 2971 (m), 2934 (m), 2873 (m), 1602 [vs, ν(C=N)], 1499 (m), 1459 (m), 1428 (m), 1400 (m), 1353 (m), 1292 (m), 1266 (m), 1196 (m), 1175 (m), 1126 (m), 1091 (w), 1044 (m), 1002 (vw), 973 (m), 945 (vw), 904 (m), 783 (w), 728 (m), 684 (w), 645 (w), 608 (m), 536 (w) cm^{-1}. $C_{13}H_{28}ClCuN_4$ (339.4 g/mol): calcd. C 46.0, H 8.3, N 16.5; found C 46.2, H 8.4, N 16.1.

[Cu(DMEGd^{i}pae)Br] (C5): Yield: 208 mg (70%). IR (KBr): $\tilde{\nu}$ = 2970 (s), 2933 (m), 2871 (m), 1602 [vs, ν(C=N)], 1498 (m), 1461 (m), 1427 (m), 1399 (m), 1352 (m), 1292 (m), 1268 (m), 1194 (m), 1172 (m), 1125 (m), 1090 (m), 1042 (m), 1000 (w), 971 (m), 941 (w), 905 (m), 781 (w), 728 (m), 684 (m), 644 (m), 608 (m), 536 (w) cm^{-1}. $C_{13}H_{28}BrCuN_4$ (383.8 g/mol): calcd. C 40.7, H 7.4, N 14.6; found C 40.7, H 7.5, N 14.6.

[Cu(DMEGd^{i}pae)I] (C6): Yield: 258 mg (60%). EI-MS: m/z (%) = 240 (16) [DMEGd^{i}pae$^+$], 197 (79) [DMEGd^{i}pae$^+$ – CH(CH$_3$)$_2$], 140 (29) [DMEGd^{i}pae$^+$ – N(CH(CH$_3$)$_2$)$_2$], 127 (73), 126 (100) [DMEGd^{i}pae$^+$ – H$_2$CN(CH(CH$_3$)$_2$)$_2^+$], 114 (78) [H$_2$CN(CH(CH$_3$)$_2$)$_2^+$], 98 (7), 84 (7), 72 (29), 56 (41), 43 (16) [CH(CH$_3$)$_2^+$], 42 (19). IR (KBr): $\tilde{\nu}$ = 2968 (m), 2919 (w), 2848 (m), 1612 [s, ν(C=N)], 1487 (m), 1458 (m), 1415 (vw), 1388 (vw), 1365 (w), 1344 (w), 1284 (m), 1263 (m), 1189 (vw), 1153 (vw), 1124 (w), 1078 (w), 1031 (vw), 973 (w), 962 (w), 908 (m) cm^{-1}. $C_{13}H_{28}CuIN_4$ (430.8 g/mol): calcd. C 36.2, H 6.6, N 13.0; found C 36.4, H 6.9, N 13.0.

[Cu(DMEGd^{i}pae)Cl$_2$] (C11): Green plates. Yield: 199 mg (53%). $C_{13}H_{28}Cl_2CuN_4$ (374.8 g/mol): calcd. C 41.7, H 7.5, N 15.0; found C 41.9, H 7.7, N 14.7.

Procedure for Styrene ATRP: The components of catalysts for polymerisation reactions containing the ligand (0.38 mmol, **L1**: 93 g, **L2**: 92 mg) and the copper salts (0.19 mmol, CuCl: 19 mg or CuBr: 27 mg) were weighed in a Schlenk flask in a glove box. For polymerisation in solution, the solvent acetonitrile was added to the catalyst. Outside the glove box first styrene (19 mmol, 2.2 mL) and finally the initiator (0.19 mmol, 1-PECl: 26 μL or 1-PEBr: 27 μL) were added through a syringe. The reaction mixture was heated in an oil bath whilst stirring for different periods of time. The poly-

merisation was stopped by cooling with liquid nitrogen. The solvents were removed under vacuum (if added). The raw polymer was precipitated in THF and eluted with THF (150 mL) through a column of neutral Al_2O_3 to remove the copper compound. After removing THF, polystyrene was added dropwise to cooled MeOH. The formed solid polystyrene was filtered and dried under vacuum. Monomer conversion was determined gravimetrically based on the isolated polystyrene.

For the kinetic studies, a mixture containing 2 mmol **L1** (484.5 mg), 1 mmol CuBr (143.5 mg) and 10 mmol styrene (10 g, 11 mL) was degassed by three freeze–thaw cycles, after which 1-PEBr (1 mmol, 178 mg, 130 μL) was added by a syringe. The polymerisation mixture was heated in an oil bath at 110 °C, and samples were taken at different time intervals and quenched by cooling with liquid nitrogen. Monomer conversion was determined by ^{1}H NMR spectroscopy, and molecular weight distributions were determined by GPC.

Supporting Information (see footnote on the first page of this article): The kinetics with the 2:1 complex, generated from one equivalent of **C2** and one additional equivalent of **L1**, figures of the geometry optimised complexes **C9***–**C20*** and simulation data for complexes **C1**–**C5** obtained with Gaussian03 are presented.

Acknowledgments

Financial support by the Fonds der Chemischen Industrie (FCI) (fellowships for S. H.-P. and O. B.) and the Bundesministerium für Bildung und Forschung (MoSGrid, 01IG09006) is gratefully acknowledged. S. H.-P. thanks Prof. K. Jurkschat for his valuable support. Calculation time is gratefully appreciated from the ARMINIUS Cluster at the PC^2 Paderborn, the SuGI Cluster at the Regionales Rechenzentrum Köln (RRZK) and the Quantix-Cluster of the work groups of Prof. Dr. M. Prosenc and Prof. Dr. P. Burger at the Universität Hamburg.

[1] R. van Eldik, J. Reedijk, "Homogeneous Biomimetic Oxidation Catalysis", *Advances in Inorganic Chemistry* ed. 1, Academic Press, **2006**.

[2] a) A. Behr, *Angewandte homogene Katalyse*, Wiley VCH, Weinheim, **2008**; b) T. Ye, A. McKervey, *Metal Catalysed Cyclopropanations*, Wiley, Chichester, **1992**; c) C. Ricardo, L. M. Matosziuk, J. D. Evanseck, T. Pintauer, *Inorg. Chem.* **2009**, *48*, 16–18.

[3] A. G. Pateman, *Copper Catalysed Aziridination Reactions*, University of London, **1999**.

[4] R. Brückner, *Reaktionsmechanismen: Organische Reaktionen, Stereochemie, moderne Synthesemethoden*, Spektrum Akademischer Verlag, Heidelberg, **1996**.

[5] a) D. P. Curran, *Comprehensive Organic Synthesis*, Pergamon, New York, **1992**; b) T. Pintauer, *Eur. J. Inorg. Chem.* **2010**, 2449–2460; c) W. T. Eckenhoff, T. Pintauer, *Catal. Rev. Sci. Eng.* **2010**, *52*, 1–59; d) T. Pintauer, K. Matyjaszewski, *Chem. Soc. Rev.* **2008**, *37*, 1087–1097.

[6] a) K. Matyjaszewski, T. P. Davis, *Handbook of Radical Polymerisation*, Wiley-Interscience, Hoboken, **2002**; b) K. Matyjaszewski, J. Xia, *Chem. Rev.* **2001**, *101*, 2921–2990.

[7] a) S. Pohl, M. Harmjanz, J. Schneider, W. Saak, G. Henkel, *J. Chem. Soc., Dalton Trans.* **2000**, 3473–3479; b) S. Pohl, M. Harmjanz, J. Schneider, W. Saak, G. Henkel, *Inorg. Chim. Acta* **2000**, *311*, 106–112.

[8] a) S. Herres, A. J. Heuwing, U. Flörke, J. Schneider, G. Henkel, *Inorg. Chim. Acta* **2005**, *358*, 1089–1095; b) S. Herres-Pawlis, A. Neuba, O. Seewald, T. Seshadri, H. Egold, U. Flörke, G. Henkel, *Eur. J. Org. Chem.* **2005**, 4879–4890; c) S. Herres-Pawlis, U. Flörke, G. Henkel, *Eur. J. Inorg. Chem.* **2005**, 3815–3824; d) S. Herres-Pawlis, P. Verma, R. Haase, P. Kang, C. T. Lyons, E. C. Wasinger, U. Flörke, G. Henkel, T. D. P. Stack, *J. Am. Chem. Soc.* **2009**, *131*, 1154–1169; e) N. Kuhn, M. Grathwohl, M. Steimann, G. Henkel, *Z. Naturforsch., Teil B* **1998**, *53*, 997–1003.

[9] a) M. Schatz, V. Raab, S. P. Foxon, G. Brehm, S. Schneider, M. Reiher, M. C. Holthausen, J. Sundermeyer, S. Schindler, *Angew. Chem.* **2004**, *116*, 4460–4463; *Angew. Chem. Int. Ed.* **2004**, *43*, 4360–4363; b) C. Würtele, E. Gaoutchenova, K. Harms, M. C. Holthausen, J. Sundermeyer, S. Schindler, *Angew. Chem.* **2006**, *118*, 3951–3953; *Angew. Chem. Int. Ed.* **2006**, *45*, 3867–3869; c) M. P. Lanci, V. V. Smirnov, C. J. Cramer, E. V. Gauchenova, J. Sundermeyer, J. P. Roth, *J. Am. Chem. Soc.* **2007**, *129*, 14697–14709; d) D. Maiti, D.-H. Lee, K. Gaoutchenova, C. Würtele, M. C. Holthausen, A. A. Narducci Sarjeant, J. Sundermeyer, S. Schindler, K. D. Karlin, *Angew. Chem.* **2008**, *120*, 88–91; *Angew. Chem. Int. Ed.* **2008**, *47*, 82–85; e) D. Maiti, D. Lee, A. A. Narducci Sarjeant, M. Y. M. Pau, E. I. Solomon, K. Gaoutchenova, J. Sundermeyer, K. D. Karlin, *J. Am. Chem. Soc.* **2008**, *130*, 6700–6701; f) J. S. Woertink, L. Tian, D. Maiti, H. R. Lucas, R. A. Himes, K. D. Karlin, F. Neese, C. Würtele, M. C. Holthausen, E. Bill, J. Sundermeyer, S. Schindler, E. I. Solomon, *Inorg. Chem.* **2010**, *49*, 9450–9459.

[10] D. Emeljanenko, A. Peters, N. Wagner, J. Beck, E. Kaifer, H.-J. Himmel, *Eur. J. Inorg. Chem.* **2010**, 1839–1846.

[11] a) H. Wittmann, A. Schorm, J. Sundermeyer, *Z. Anorg. Allg. Chem.* **2000**, *626*, 1583–1590; b) H. Wittmann, V. Raab, A. Schorm, J. Plackmeyer, J. Sundermeyer, *Eur. J. Inorg. Chem.* **2001**, 1937–1846; c) V. Raab, J. Kipke, O. Burghaus, J. Sundermeyer, *Inorg. Chem.* **2001**, *40*, 6964–6971.

[12] a) M. P. Coles, *Dalton Trans.* **2006**, 985–1001; b) S. H. Oakley, D. B. Soria, M. P. Coles, P. B. Hitchcock, *Dalton Trans.* **2004**, 537–546; c) S. H. Oakley, M. P. Coles, P. B. Hitchcock, *Inorg. Chem.* **2003**, *42*, 3154–3156.

[13] a) A. Neuba, O. Seewald, U. Flörke, G. Henkel, *Acta Crystallogr., Sect. E* **2007**, *63*, m2099–u697; b) S. Herres-Pawlis, R. Haase, E. Akin, U. Flörke, G. Henkel, *Z. Anorg. Allg. Chem.* **2008**, *634*, 295–298; c) S. Herres, U. Flörke, G. Henkel, *Acta Crystallogr., Sect. C* **2004**, *60*, m659–m660; d) S. Herres-Pawlis, U. Flörke, G. Henkel, *Acta Crystallogr., Sect. E* **2005**, *61*, m79–m81; e) S. Herres-Pawlis, U. Flörke, G. Henkel, *Acta Crystallogr., Sect. E* **2006**, *62*, m2138–m2140; A. Neuba, R. Haase, M. Bernard, U. Flörke, S. Herres-Pawlis, *Z. Anorg. Allg. Chem.* **2008**, *634*, 2511–2517; f) A. Neuba, S. Herres-Pawlis, O. Seewald, J. Börner, A. J. Heuwing, U. Flörke, G. Henkel, *Z. Anorg. Allg. Chem.* **2010**, *636*, 2641–2649; g) R. Wortmann, U. Flörke, B. Sarkar, V. Umamaheshwari, G. Gescheidt, S. Herres-Pawlis, G. Henkel, *Eur. J. Inorg. Chem.* **2011**, 121–130.

[14] a) U. Wild, O. Hübner, A. Maronna, M. Enders, E. Kaifer, H. Wadepohl, H.-J. Himmel, *Eur. J. Inorg. Chem.* **2008**, *28*, 4440–4447; b) A. Peters, C. Trumm, M. Reinmuth, D. Emeljanenko, E. Kaifer, H.-J. Himmel, *Eur. J. Inorg. Chem.* **2009**, *25*, 3791–3800; c) M. Reinmuth, U. Wild, E. Kaifer, M. Enders, H. Wadepohl, H.-J. Himmel, *Eur. J. Inorg. Chem.* **2009**, 4795–4808; d) P. Roquette, A. Maronna, A. Peters, E. Kaifer, H.-J. Himmel, C. Hauf, V. Herz, E.-W. Scheidt, W. Scherer, *Chem. Eur. J.* **2010**, *16*, 1336–11350; e) V. Vitske, C. König, O. Hübner, E. Kaifer, H.-J. Himmel, *Eur. J. Inorg. Chem.* **2010**, 115–126; f) A. Peters, U. Wild, O. Hübner, E. Kaifer, H.-J. Himmel, *Chem. Eur. J.* **2008**, *14*, 7813–7821; g) V. Vitske, C. König, O. Hübner, E. Kaifer, H.-J. Himmel, *Eur. J. Inorg. Chem.* **2009**, 115–126.

[15] a) R. Wortmann, A. Hoffmann, R. Haase, U. Flörke, S. Herres-Pawlis, *Z. Anorg. Allg. Chem.* **2009**, *635*, 64–69; b) J. Börner, S. Herres-Pawlis, U. Flörke, K. Huber, *Eur. J. Inorg. Chem.* **2007**, 5645–5651; c) J. Börner, U. Flörke, K. Huber, A. Döring, D. Kuckling, S. Herres-Pawlis, *Chem. Eur. J.* **2009**, *15*, 2362–2376; d) A. Hoffmann, J. Börner, U. Flörke, S. Herres-Pawlis, *Inorg. Chim. Acta* **2009**, *362*, 1185–1193.

[16] a) J.-S. Wang, K. Matyjaszewski, *J. Am. Chem. Soc.* **1995**, *117*, 5614–5615; b) M. Kato, M. Kamigaito, M. Sawamoto, T. Higa-

shimura, *Macromolecules* **1995**, *28*, 1721–1723; c) T. E. Patten, J. Xia, T. Abernathy, K. Matyjaszewski, *Science* **1996**, *272*, 866–868; d) T. E. Patten, K. Matyjaszewski, *Adv. Mater.* **1998**, *10*, 901–915; e) V. Coessens, T. Pintauer, K. Matyjaszewski, *Prog. Polym. Sci.* **2001**, *26*, 337–377.

[17] a) K. Matyjaszewski, J. Xia, *Chem. Rev.* **2001**, *101*, 2921–2990; b) M. Kamigaito, T. Ando, M. Sawamoto, *Chem. Rev.* **2001**, *101*, 3689–3945; F. Simal, A. Demonceau, A. F. Noals, *Angew. Chem.* **1999**, *111*, 559–562; *Angew. Chem. Int. Ed.* **1999**, *38*, 538–541; c) K. Matyjaszewski, M. Wei, J. Xia, N. E. McDermott, *Macromolecules* **1997**, *30*, 8161–8164; d) T. Ando, M. Kamigaito, M. Sawamoto, *Macromolecules* **1997**, *30*, 4507–4510; e) B. Göbelt, K. Matyjaszewski, *Macromol. Chem. Phys.* **2000**, *201*, 1619–1624.

[18] a) W. Tang, Y. Kwak, W. Braunecker, N. V. Tsarevsky, M. L. Coote, K. Matyjaszewski, *J. Am. Chem. Soc.* **2008**, *130*, 10702–10713; b) J. Xia, X. Zhang, K. Matyjaszewski, *ACS Symp., Ser.* **2000**, *760*, 207–223; c) D. M. Haddleton, C. Waterson, P. J. Derrick, C. B. Jasieczek, A. J. Shooter, *Chem. Commun.* **1997**, 683–684; d) D. M. Haddleton, A. J. Clark, M. C. Crossman, D. J. Dunclaf, A. M. Heming, S. R. Morsley, A. J. Shooter, *Chem. Commun.* **1997**, 1173–1174.

[19] a) O. Bienemann, R. Haase, U. Flörke, A. Döring, D. Kuckling, S. Herres-Pawlis, *Z. Naturforsch., Teil B* **2010**, *65*, 798–806; b) D. Petrovic, L. M. R. Hill, P. G. Jones, W. B. Tolman, M. Tamm, *Dalton Trans.* **2008**, 887–894.

[20] N. Kenichi, *Jpn. Kokai Tokkyo Koho* **2002**, JP 2002148749 A 20020522.

[21] W. Kantlehner, E. Haug, W. W. Mergen, P. Speh, T. Maier, J. J. Kapassakalidis, H.-J. Bräuner, H. Hagen, *Liebigs Ann. Chem.* **1984**, *1*, 108–125.

[22] $\rho = 2a/(b + c)$; $a = d(C_{gua}{=}N_{gua})$, b and $c = d(C_{gua}{-}N_{amine,gua})$.

[23] a) V. Raab, K. Harms, J. Sundermeyer, B. Kovacevic, Z. B. Maksic, *J. Org. Chem.* **2003**, *68*, 8790–8797; b) S. Herres-Pawlis, T. Seshadri, U. Flörke, G. Henkel, *Z. Anorg. Allg. Chem.* **2009**, *635*, 1209–1214.

[24] R. Haase, Dissertation, University of Paderborn, Paderborn, **2010**.

[25] J. P. Perdew, *Phys. Rev. B* **1986**, *33*, 8822–8824; J. P. Perdew, *Phys. Rev. B* **1986**, *34*, 7406–7406.

[26] F. Weigend, M. Häser, H. Patzelt, R. Ahlrichs, *Chem. Phys. Lett.* **1998**, *294*, 143–152.

[27] a) TURBOMOLE V6.1, **2009**, University of Karlsruhe and Forschungszentrum Karlsruhe GmbH, **1989–2007**, Turbomole GmbH (since **2007**); b) K. Eichkorn, O. Treutler, H. Öhm, M. Häser, R. Ahlrichs, *Chem. Phys. Lett.* **1995**, *242*, 652–660.

[28] J. Xia, K. Matyjaszewski, *Macromolecules* **1997**, *30*, 7697–7700.

[29] J.-L. Wang, T. Grimaud, K. Matyjaszewski, *Macromolecules* **1997**, *30*, 6507–6512.

[30] K. Matyjaszewski, T. E. Patten, J. Xia, *J. Am. Chem. Soc.* **1997**, *119*, 674–680.

[31] J. Leonard, B. Lygo, G. Procter, *Praxis der Organischen Chemie*, VCH, Weinheim, **1996**.

[32] *SMART (Version 5.62), SAINT (Version 6.02), SHELXTL (Version 6.10) and SADABS (Version 2.03)*, Bruker AXS Inc., Madison, Wisconsin, **2002**.

[33] M. J. Frisch, G. W. Trucks, H. B. Schlegel, G. E. Scuseria, M. A. Robb, J. R. Cheeseman, J. A. Montgomery Jr., T. Vreven, K. N. Kudin, J. C. Burant, J. M. Millam, S. S. Iyengar, J. Tomasi, V. Barone, B. Mennucci, M. Cossi, G. Scalmani, N. Rega, G. A. Petersson, H. Nakatsuji, M. Hada, M. Ehara, K. Toyota, R. Fukuda, J. Hasegawa, M. Ishida, T. Nakajima, Y. Honda, O. Kitao, H. Nakai, M. Klene, X. Li, J. E. Knox, H. P. Hratchian, J. B. Cross, C. Adamo, J. Jaramillo, R. Gomperts, R. E. Stratmann, O. Yazyev, A. J. Austin, R. Cammi, C. Pomelli, J. W. Ochterski, P. Y. Ayala, K. Morokuma, G. A. Voth, P. Salvador, J. J. Dannenberg, V. G. Zakrzewski, S. Dapprich, A. D. Daniels, M. C. Strain, O. Farkas, D. K. Malick, A. D. Rabuck, K. Raghavachari, J. B. Foresman, J. V. Ortiz, Q. Cui, A. G. Baboul, S. Clifford, J. Cioslowski, B. B. Stefanov, G. Liu, A. Liashenko, P. Piskorz, I. Komaromi, R. L. Martin, D. J. Fox, T. Keith, M. A. Al-Laham, C. Y. Peng, A. Nanayakkara, M. Challacombe, P. M. W. Gill, B. Johnson, W. Chen, M. W. Wong, C. Gonzalez, and J. A. Pople, *Gaussian 03, Revision E.01*, Gaussian, Inc., Wallingford CT, **2004**.

[34] a) A. D. Becke, *J. Chem. Phys.* **1993**, *98*, 5648; b) C. Lee, W. Yang, R. G. Parr, *Phys. Rev. B* **1988**, *37*, 785; c) B. Miehlich, A. Savin, H. Stoll, H. Preuss, *Chem. Phys. Lett.* **1989**, *157*, 200.

[35] F. Weinhold, C. Landis, *Valency and Bonding – A Natural Bond Orbital Donor-Acceptor Perspective*, Cambridge University Press, New York, **2005**.

[36] a) W. A. Braunecker, W. C. Brown, B. C. Morelli, W. Tang, R. Poli, K. Matyjaszewski, *Macromolecules* **2007**, *40*, 8576–8585; b) A. Révész, P. Milko, J. Zabka, D. Schröder, J. Roithová, *J. Mass Spectrom.* **2010**, *45*, 1246–1252.

Received: November 12, 2010
Published Online: April 8, 2011

